RESEARCH ARTICLE

Key Points:
- The formation mechanisms of several major carbonyls in Beijing were diagnosed by field observations coupled with an MCM box model
- Alkenes are the principal precursors of $HCHO$ and CH_3CHO, while aromatics and BVOCs are the major precursors of glyoxal and MGLY in Beijing
- Carbonyls play a significant role in the atmospheric oxidizing capacity, RO_x radical chemistry, and O_3 pollution in Beijing

Observations and Explicit Modeling of Summertime Carbonyl Formation in Beijing: Identification of Key Precursor Species and Their Impact on Atmospheric Oxidation Chemistry

Xue Yang[1,2], Likun Xue[1] iD, Tao Wang[1,2,3] iD, Xinfeng Wang[1] iD, Jian Gao[3], Shuncheng Lee[2], Donald R. Blake[4], Fahe Chai[3], and Wenxing Wang[1,3]

[1]Environment Research Institute, Shandong University, Ji'nan, China, [2]Department of Civil and Environmental Engineering, Hong Kong Polytechnic University, Hong Kong, [3]Chinese Research Academy of Environmental Sciences, Beijing, China, [4]Department of Chemistry, University of California, Irvine, CA, USA

Abstract Carbonyls are an important group of volatile organic compounds (VOCs) that play critical roles in tropospheric chemistry. To better understand the formation mechanisms of carbonyl compounds, extensive measurements of carbonyls and related parameters were conducted in Beijing in summer 2008. Formaldehyde (11.17 ± 5.32 ppbv), acetone (6.98 ± 3.01 ppbv), and acetaldehyde (5.27 ± 2.24 ppbv) were the most abundant carbonyl species. Two dicarbonyls, glyoxal (0.68 ± 0.26 ppbv) and methylglyoxal (MGLY; 1.10 ± 0.44 ppbv), were also present in relatively high concentrations. An observation-based chemical box model was used to simulate the in situ production of formaldehyde, acetaldehyde, glyoxal, and MGLY and quantify their contributions to ozone formation and RO_x budget. All four carbonyls showed similar formation mechanisms but exhibited different precursor distributions. Alkenes (mainly isoprene and ethene) were the dominant precursors of formaldehyde, while both alkenes (e.g., propene, i-butene, and cis-2-pentene) and alkanes (mainly i-pentane) were major precursors of acetaldehyde. For dicarbonyls, both isoprene and aromatic VOCs were the dominant parent hydrocarbons of glyoxal and MGLY. Photolysis of oxygenated VOCs was the dominant source of RO_x radicals (approximately >80% for HO_2 and approximately >70% for RO_2) in Beijing. Ozone production occurred under a mixed-control regime with carbonyls being the key VOC species. Overall, this study provides some new insights into the formation mechanisms of carbonyls, especially their parent hydrocarbon species, and underlines the important role of carbonyls in radical chemistry and ozone pollution in Beijing. Reducing the emissions of alkenes and aromatics would be an effective way to mitigate photochemical pollution in Beijing.

1. Introduction

Carbonyl compounds, such as aldehydes, ketones, and dicarbonyls, are ubiquitous in the troposphere and have a critical influence on atmospheric chemistry. The photolysis of carbonyl compounds is a significant source of radicals and hence determines the atmospheric oxidizing capacity (Liu, Wang, Gu, et al., 2012; Xue et al., 2016). As an important class of reactive volatile organic compounds (VOCs), carbonyls are principal precursors of ozone (O_3) and secondary organic aerosols (SOAs) (Atkinson, 2000; Fu et al., 2008; Rao et al., 2016; Xue et al., 2016). High concentrations of carbonyls, such as formaldehyde (HCHO) and acetaldehyde (CH_3CHO), can cause detrimental effects (e.g., carcinogenic risks) to human health (Huang et al., 2011). Carbonyls are important products from the oxidation of various hydrocarbons (Atkinson, 2000) and can also be emitted directly from the combustion of fossil fuels, natural vegetation, and biomass (Liu et al., 2009; Mason et al., 2001). Hence, pollution by carbonyls has attracted much attention in recent years given their significant role in atmospheric chemistry, health risks, and the complexity of their formation mechanisms.

Previous work has reported on the serious carbonyl pollution in China as a result of its rapid industrialization and urbanization. Numerous measurements of ambient carbonyls have been conducted, focusing on the pollution levels and potential sources of formaldehyde and acetaldehyde in the urban atmosphere (Duan et al., 2012; Li et al., 2010; Ling et al., 2016; Lü et al., 2009; Yang et al., 2017; Yuan et al., 2012). For example, Liu et al. (2009) reported high levels of oxygenated VOCs (OVOCs) in Beijing and apportioned about half of the acetaldehyde to secondary sources with a least squares linear-fit approach. In the Yangtze River Delta (YRD) region of eastern China, Wang et al. (2015) reported that about 34.9% of the measured HCHO was

attributable to photochemical production. In comparison with HCHO and CH₃CHO, less attention has been paid to the dicarbonyls, such as glyoxal (CHOCHO) and methyl glyoxal (MGLY), which are important precursors of O_3 and SOAs (Fu et al., 2008; Ho et al., 2014; Lim et al., 2013; Liu et al., 2010; Liu, Wang, Vrekoussis, et al., 2012). Indeed, Chan Miller et al. (2016) identified the Pearl River Delta (PRD) region as a hot spot for CHOCHO from the Ozone Monitoring Instrument satellite observations. Li et al. (2014) also observed high concentrations of CHOCHO at a semirural site in the PRD. More efforts are needed to shed light on the characteristics and formation mechanisms of dicarbonyls, especially in the major industrialized regions of China, such as the PRD, YRD, and North China Plain.

Considering the remarkable contribution of secondary formation to ambient carbonyls, a detailed understanding of their formation chemistry and precursors is essential to establish effective measures to control carbonyl pollution. It has been shown that these carbonyl compounds are produced via the oxidation reaction chains of various hydrocarbons, and the dominant primary precursors are quite inhomogeneous between different carbonyl species and different study areas. In remote areas, HCHO production is mainly attributable to the methane (CH_4) oxidation reaction by OH radicals, whereas in semirural areas, it is dominated by isoprene (C_5H_8) degradation (Li et al., 2014). In comparison, in urban areas, anthropogenic alkenes are usually important precursors of HCHO (Liu et al., 2015). Anthropogenic alkenes and alkanes dominate the secondary production of CH₃CHO (Liu et al., 2015). Globally, the oxidation of isoprene and ethyne are the major formation pathways of CHOCHO and MGLY (Fu et al., 2008). However, in the polluted PRD area, anthropogenic aromatics are proposed to be the major precursors of CHOCHO (Chan Miller et al., 2016; Li et al., 2014; Liu, Wang, Vrekoussis, et al., 2012). Obviously, identification of the parent hydrocarbon species and quantification of the carbonyl-precursor relationships are essential prerequisites for understanding carbonyl formation and developing pollution control strategies.

Rapid industrialization and urbanization has also led to severe ozone air pollution in China, with surface O_3 concentrations frequently exceeding the national ambient air quality limits (Wang et al., 2006, 2016; Xue et al., 2011; Xue, Wang, Gao, et al., 2014; Xue, Wang, Louie, et al., 2014). Over the past decade, the continuously improving knowledge of the O_3-precursor relationship has supported the formulation of antipollution strategies (Chou et al., 2011; Xue, Wang, Gao, et al., 2014). For instance, considering the VOC-limited regime of O_3 formation in many urban areas, such as Beijing, Shanghai, and Guangzhou, the key VOC groups contributing the most to O_3 formation have been further assessed and subjected to a series of strict control measures (Cheng et al., 2010; Huang et al., 2008; Xu et al., 2011; Xue, Wang, Gao, et al., 2014). However, these studies have mainly focused on hydrocarbons, with only occasional attention being paid to carbonyls because of the limited observational data. A recent study has indicated the dominant role of OVOCs in the radical sources ($RO_x = OH + RO_2 + HO_2$) in the polluted Hong Kong and PRD region (Xue et al., 2016). These RO_x radicals can dominate the atmospheric oxidative capacity (AOC) and thus govern the O_3 formation (Hofzumahaus et al., 2009). Consequently, the quantitative effects of carbonyls on O_3 formation, atmospheric oxidizing capacity, and radical chemistry require further evaluation to comprehensively understand the cause of the O_3 problem.

In this study, to better understand the chemical cause of photochemical pollution, we investigate the formation mechanism of major carbonyls in Beijing during the summer of 2008. We first show the concentration levels and chemical compositions of the observed carbonyls. We then analyze the photochemical formation processes of HCHO, CH₃CHO, CHOCHO, and MGLY, with the application of an observation-based chemical box model constrained by a full suite of observed chemical species and meteorological parameters. Through this detailed chemical analysis, we have aimed to explicitly explore the dominant formation pathways and the primary precursor species of carbonyls. Sensitivity experiments were conducted to diagnose the formation regimes of major carbonyls. Finally, we elaborate on the impacts of carbonyl compounds on O_3 formation and the RO_x chemical budget in Beijing.

2. Materials and Methods

2.1. Experiments

The field experiments were conducted on the rooftop of a three-story building (15 m above the ground level) in the Chinese Research Academy of Environmental Sciences (CRAES). This is a suburban site situated in the northern part of the center of Beijing and closed to the fifth ring road (see Figure 1). When southerly winds
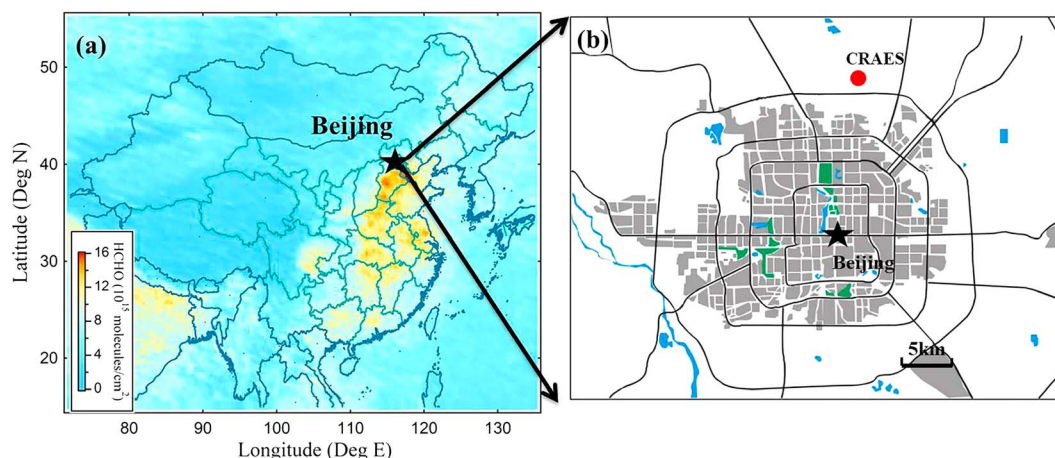
Figure 1. (a) Map showing the location of Beijing and satellite-retrieved (GOME-2(B)) summertime (June-July-August) average HCHO column densities in 2008 and (b) location of the sampling site (CRAES) in Beijing.

prevail, it is normally located downwind of downtown Beijing. Detailed information about this site has been described elsewhere (Wang et al., 2010; Xue, Wang, Wang, et al., 2014).

The concentrations of carbonyls, methane (CH_4), and nonmethane hydrocarbons (NMHCs) were determined simultaneously on high O_3 episode days from 16 July to 26 August 2008. There was at least one sample on each selected O_3 episode day. In addition, to capture the contributions of photochemical reactions to carbonyls and O_3 pollution, there were more samples (up to seven) on particular episode days (Wang et al., 2010). Ambient carbonyl samples were collected by drawing ambient air through a 2,4-dinitrophenylhydrazine-coated sorbent cartridge. The samples were taken from 07:00 to 19:00 local time (LT) with a flow rate of 1 L min^{-1} and a duration of 2 h. A total of 94 samples were obtained during the field campaign. After sampling, a high-performance liquid chromatography (PerkinElmer Series 2000) system was used for the detection of carbonyl species in the air laboratory of the Hong Kong Polytechnic University (Ho & Yu, 2004; Xue, Wang, Wang, et al., 2014). In total, 17 carbonyl species were identified and quantified in this study. CH_4 and NMHCs were sampled by taking whole ambient air in 2 L stainless steel canisters and analyzed using a five-column multiple gas chromatograph (GC) system equipped with flame ionization detector, mass spectrometry detector, and electron capture detector (ECD) at the University of California at Irvine, with a detection limit of 3 pptv for all quantified VOC species (Simpson et al., 2010). The samples were taken every 2 h from 07:00 to 19:00 LT with a duration of 2 min. In total, 109 canister samples were taken during the sampling period.

The concentrations of O_3, NO, NO_2, NO_y, and peroxyacetyl nitrate (PAN) and the meteorological parameters, including ambient temperature, relative humidity (RH), wind speed and direction, and total ultraviolet radiation, were continuously monitored with a set of commercial instruments. Brief descriptions are as follows. O_3 was determined using a commercial ultraviolet absorption analyzer (TEI model 49i), CO using a nondispersive infrared analyzer (API model 300EU), NO_x and NO_y using a chemiluminescence method (TEI model 42i and TEI model 42cy, equipped with a blue light converter and molybdenum oxide converter, respectively), and PAN using a commercial GC-ECD analyzer (Meteorologie Consult GmbH). The details of the calibration and quality assurance of the above instruments can be found elsewhere (Wang et al., 2001; Xue, Wang, Wang, et al., 2014).

2.2. Observation-Based Model

The observation-based model for investigating atmospheric oxidative capacity and photochemistry (OBM-AOCP) has proved to be a robust tool for explicit simulation of atmospheric chemistry. It has been extensively applied to simulate O_3 formation (Xue et al., 2013; Xue, Wang, Gao, et al., 2014), PAN production (Xue, Wang, Wang, et al., 2014), atmospheric oxidative capacity, and RO_x chemistry (Xue et al., 2016). In this study, the model was updated to the newest version of the Master Chemical Mechanism (MCM, v3.3; http://mcm.leeds.ac.uk/MCM/). This nearly explicit mechanism uses about 17,000 reactions of approximately 6,700

species plus the latest International Union of Pure and Applied Chemistry inorganic chemistry evaluation inorganic chemistry evaluation (Jenkin et al., 2003; Jenkin, Young, & Rickard, 2015; Saunders et al., 2003). In addition to the homogeneous chemistry, heterogeneous chemical processes, dry deposition, and dilution mixing within the boundary layer are also considered in this model. A detailed description of the configuration and validation of this model has been provided elsewhere (Xue, Wang, Gao, et al., 2014; Xue et al., 2016) and is also documented in the supporting materials (Zhang et al., 2003).

In this study, the OBM-AOCP model was applied to simulate the photochemical production and destruction of major carbonyls (i.e., HCHO, CH_3CHO, CHOCHO, and MGLY) and O_3 and to elucidate the AOC and RO_x budget in Beijing. The calculation of ozone production rates and RO_x budget has been described elsewhere (Xue et al., 2013; Xue, Wang, Wang, et al., 2014; Xue et al., 2016). Here we introduce the computation of reaction rates of secondary carbonyls in detail. In the troposphere, secondary carbonyls are formed through a variety of reactions. Specifically, 399, 163, 149, and 202 chemical reactions are related to the formation of HCHO, CH_3CHO, CHOCHO, and MGLY, respectively, in the MCM. These reactions were explicitly tracked in our model and grouped into several major production routes: reactions of $RO + O_2$, photolysis of OVOCs, O_3 + OVOCs, OH + OVOCs, and propagation of radicals (i.e., mutual reactions of RCO_3, HO_2, NO_3, and RO_2 radicals to produce carbonyls). The production rate of carbonyls can be obtained by adding these reaction rates together. In addition to the formation processes, the destruction routes of carbonyls were also tracked. In general, the chemical loss of carbonyls was dominated by reactions with OH and NO_3 and photolysis. The carbonyl destruction rates can be calculated as the sum of these loss rates. Thus, the net production rate of carbonyls (Net P(carbonyls)) can be quantified by the difference between the production rate (P(carbonyls)) and the loss rate (L(carbonyls)).

In the calculations, the observed concentrations of O_3, SO_2, CO, NO, NO_2, CH_4, C_2–C_{10} NMHCs, carbonyls, H_2O, temperature, and J_{NO2} were averaged or interpolated to a time resolution of 1 h and processed as the model input data sets. For the data gaps of hydrocarbons and carbonyls, which were not measured in real time, the time-dependent data were linearly interpolated during the intensively collected time (i.e., 07:00 to 19:00 LT), whereas the other nighttime data were calculated according to the linear regressions with temperature for isoprene, and with CO for CH_4 and C_2–C_{10} NMHC species (Xue, Wang, Wang, et al., 2014). In particular, for carbonyls, the nighttime data were obtained by a multilinear regression fit model with O_3 and CO as tracers to account for the primary and secondary sources. The model calculation was made for several particular photochemical pollution cases (i.e., 23 and 24 July and 13 and 20 August 2008), for which O_3 existed at relatively high concentrations and detailed measurements of carbonyls and NMHCs were available. The time of 00:00 LT was set as the initial time, and the integration over 24 h was conducted with an integration step of 1 h. The integration was conducted five times in series, and the results of the fifth run were used as the output of the simulation ascribed to the steady state of unconstrained species (e.g., radicals).

The modeling analyses were inherently subject to some uncertainties, which are related to several key parameters such as the ambient concentrations of reactive species, photolysis frequencies, dry deposition, and boundary layer height. In the present study, the box model was constrained by a detailed set of field measurement data and based on the state-of-the-art chemistry to calculate the rates of particular chemical reactions and to evaluate the sensitivity of carbonyl formation to its individual precursor species. Photolysis frequencies (J values) were first simulated by the model and then scaled by the measured J_{NO2} to present the realistic atmospheric conditions. Some recent studies have suggested that the chemistry of OH has not been fully understood in this region (Lu et al., 2013; Tan et al., 2017). To check the potential impact of the OH chemistry, we conducted sensitivity modeling analyses by adding a small amount of HONO (as a primary OH source) or NO (to account for the unrecognized OH regeneration mechanism) and found that their impacts on the modeling results were relatively small. The sensitivity modeling results are documented in the supporting information (Lu et al., 2013; Tan et al., 2017; Tham et al., 2017).

3. Results and Discussion

3.1. Concentration Levels and Chemical Compositions

Figure 2 shows the measured time series of the major carbonyl compounds, O_3, CO, NO_2, NO_y, and meteorological parameters in Beijing over the period from 16 July to 26 August 2008. Clearly, severe photochemical
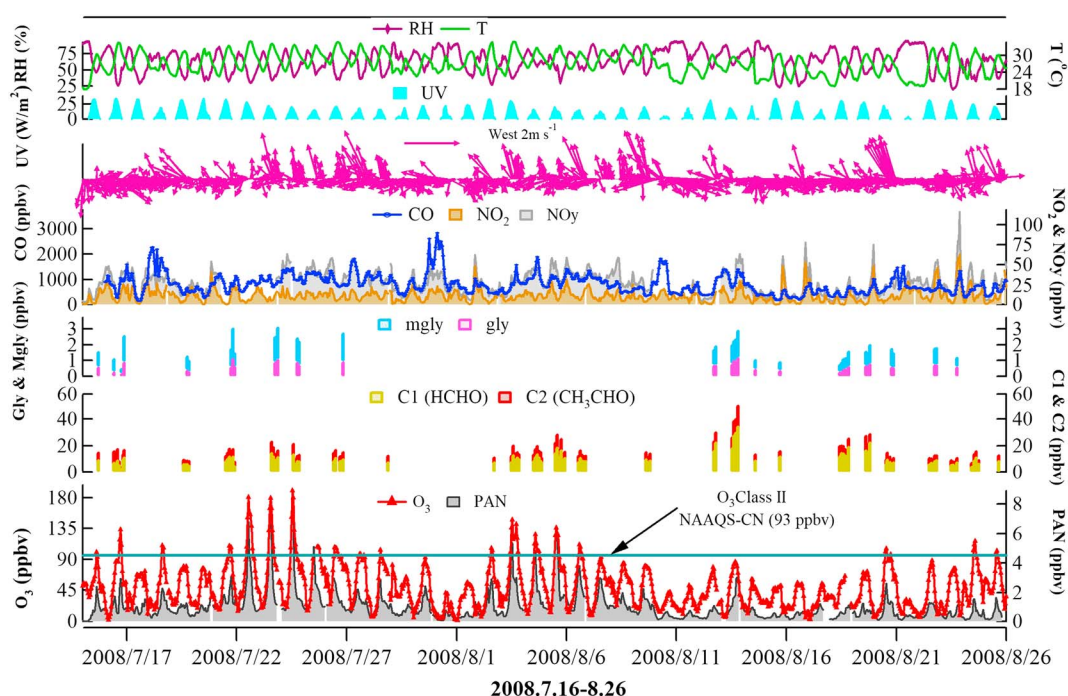
Figure 2. Time series of major carbonyl compounds, related trace gases, and meteorological parameters at CRAES between 16 July and 26 August 2008.

air pollution, as indicated by high concentrations of O_3 and PAN, was encountered during the early stages of the investigation period (e.g., 22 to 25 July) with higher temperatures and lower RH. The levels of carbonyls were also very high, with peak values of 1.21 ppbv and 2.03 ppbv recorded for CHOCHO and MGLY, respectively, in the late afternoon (17:00 LT) of 23 July. In comparison, reasonable air quality was observed during the later period with lower concentrations of O_3, PAN, and carbonyls (with the exception of 13 August), which can be ascribed to the different weather conditions (frequent rainfall and lower temperature) (Wang et al., 2010). However, the peak HCHO and CH_3CHO values (35.08 and 15.82 ppbv) were observed on 13 August, which may be interpreted as acute irregular emissions surrounding the sampling site, given the weakened local photochemistry with lower UV levels and temperatures. In addition, clear day-to-day variation patterns of O_3 and carbonyl concentrations with nearly simultaneous peaks at noon were seen, which demonstrates the contribution of photooxidation reactions to O_3 and carbonyls in the daytime. These observations highlight the severe photochemical air pollution during the pollution episodes in Beijing and indicate the secondary sources of the observed O_3 and carbonyls.

Table 1 lists the statistical results of the measurement data for the top 10 carbonyl species and related pollu-tants during the whole investigation. The average total concentration (±standard deviation) of these carbonyl compounds was 28.49 ± 10.64 ppbv, with a range from 7.96 to 76.09 ppbv. HCHO was the most abundant carbonyl, with an average value of 11.17 ± 5.32 ppbv and ranging from 3.14 to 35.08 ppbv, and accounted for 39.2% of the measured top 10 carbonyls. Such levels of HCHO in Beijing are comparable to those mea-sured in Guangzhou (10.9 ppbv) (Lü et al., 2009) but two to four times higher than those measured in other urban areas, for example, 4.62 ppbv in Nanjing (Guo et al., 2016) and 2.9 ppbv in Hong Kong (Ling et al., 2016). Acetone was the second most abundant carbonyl (6.98 ± 3.01 ppbv), followed by CH_3CHO (5.27 ± 2.24 ppbv). It is clear that HCHO, acetone, and CH_3CHO were the principal carbonyl compounds, accounting for approxi-mately 82% of the total top 10 carbonyls. Interestingly, in addition to these three abundant carbonyls discussed above, two dicarbonyls, CHOCHO and MGLY, also presented abundant levels (0.68 ± 0.26 and 1.10 ± 0.44 ppbv, respectively) despite their high reactivity. These two dicarbonyls have been pointed out as important precursors of SOAs and O_3 (Fu et al., 2008; Ho et al., 2014). However, the concentration levels and formation mechanisms of these two dicarbonyls in China have not been thoroughly understood. Ho et al. (2014) reported the levels of CHOCHO (0.23 ppbv) and MGLY (0.30 ppbv) in summer in urban Xi'an, which were much lower than those measured in the present study in Beijing. In the following sections, we

Table 1
Statistics of the Top 10 Carbonyl Compounds and Related Pollutants Measured in Beijing From 16 July to 26 August 2008[a]

Compound	Mean ± SD	Range	Compound	Mean ± SD (ppbv)	Range
CO	634 ± 268	139–1,570	n-Octane	49 ± 41	6–319
O_3	49 ± 31	1–190	n-Nonane	44 ± 30	4–163
NOx	13.10 ± 8.21	1.37–88.38	2,2-Dimethylbutane	57 ± 30	12–197
HCHO	11.17 ± 5.32	3.14–35.08	2,3-Dimethylbutane	224 ± 132	26–716
Acetone	6.98 ± 3.01	2.44–22.15	2-Methylpentane	420 ± 237	30–1,408
CH_3CHO	5.27 ± 2.24	1.73–15.82	3-Methylpentane	262 ± 173	22–965
MGLY	1.10 ± 0.44	0.34–2.03	2-Methylhexane	148 ± 92	8–529
CHOCHO	0.68 ± 0.26	0.20–1.20	3-Methylhexane	184 ± 112	42–608
Methyl ethyl ketone	0.66 ± 0.39	BDL[b]–2.15	2,4-Dimethylpentane	269 ± 224	23–1,955
Isovaleraldehyde	0.59 ± 0.51	BDL–2.10	2,3-Dimethylpentane	38 ± 31	4–229
iso- + n-butyraldehyde	0.40 ± 0.22	BDL–1.49	2,2,4-Trimethylpentane	66 ± 158	4–1,323
Nonanaldehyde	0.40 ± 0.30	BDL–1.27	2,3,4-Trimethylpentane	24 ± 58	3–401
Propionaldehyde	0.36 ± 0.21	BDL–1.23	Cyclopentane	69 ± 43	9–216
Total OVOCs	28.49 ± 10.64	7.96–76.09	Methylcyclopentane	31 ± 22	4–138
Isoprene	1,575 ± 1,283	82–7,591	Cyclohexane	109 ± 102	12–575
Ethene	1,965 ± 1,362	285–7,664	Methylcylohexane	61 ± 54	3–299
Propene	274 ± 234	35–1,473	i-Pentane	1,801 ± 1,350	177–11,565
1-Butene	258 ± 239	32–1,540	n-Pentane	592 ± 424	54–1,957
trans-2-Butene	83 ± 80	8–468	Benzene	1,244 ± 717	99–3,778
cis-2-Butene	80 ± 72	10–408	Toluene	1,681 ± 1,578	174–12,341
1,3-Butadiene	36 ± 39	4–246	Ethylbenzene	439 ± 329	49–1,857
trans-2-Pentene	49 ± 46	3–344	m + p-Xylene	581 ± 494	70–2,919
2-Methyl-1-butene	66 ± 51	6–307	o-Xylene	172 ± 152	14–908
CH_4	2.20 ± 0.38	1.89–4.48	i-Propylbenzene	23 ± 13	4–77
Ethyne	2,719 ± 1,565	224–7,613	n-Propylbenzene	32 ± 28	4–233
Ethane	3,401 ± 1,826	950–8,810	3-Ethyltoluene	65 ± 65	6–517
Propane	2,189 ± 1,676	256–7,994	4-Ethyltoluene	36 ± 42	3–369
i-Butane	1,687 ± 2,019	177–20,805	2-Ethyltoluene	33 ± 37	3–323
n-Butane	1,535 ± 1,128	116–5,437	1,3,5-Trimethylbenzene	22 ± 42	3–388
n-Hexane	329 ± 260	24–1,571	1,2,4-Trimethylbenzene	71 ± 102	6–918
n-Heptane	119 ± 86	7–423	1,2,3-Trimethylbenzene	29 ± 62	3–581

[a]Values are mean concentrations ± standard deviations in pptv; CO, O_3, NO_x, and carbonyls in ppbv; CH_4 in ppmv.   [b]BDL: below detection limit

will focus on the formation mechanisms of four abundant and reactive carbonyls, i.e., HCHO, CH_3CHO, CHOCHO, and MGLY.

3.2. Formation Mechanisms and Principal Precursors of Major Carbonyls

To dissect the photochemical formation mechanisms of the major carbonyls in Beijing, detailed modeling analyses were conducted to identify the major formation pathways and principal precursor species of HCHO, CH_3CHO, CHOCHO, and MGLY. Four photochemical pollution cases (i.e., 23 and 24 July and 13 and 20 August 2008) were selected as representative cases for which detailed measurements of hydrocarbons and carbonyls were available. Examination of the NO_2/NO and NO_x/NO_y ratios in these cases suggested that the air masses sampled during the daytime were rather photochemically aged (see Figure S8 in the supporting information), and hence, secondary formation is expected to be significant. In general, the modeling results among different cases were consistent with each other, and thus, only the results on 23 and 24 July 2008 were shown in the context, with the results of the other cases provided in the supporting materials (Figures S9–S13).

3.2.1. In Situ Formation Pathways

According to the MCM, there are five main types of reactions for the in situ formation of carbonyls, specifically, OVOC photolysis, O_3 + OVOCs, OH + OVOCs, radical propagation reactions, and RO + O_2 reactions. Overall, we found that RO + O_2 reactions made the dominant contribution to the formation of HCHO and CH_3CHO and RO + O_2 and OH + OVOC reactions made comparable contributions to the formation of CHOCHO and MGLY. Considering the dominant role of the RO + O_2 and OH + OVOCs pathways, further refinement and classification was conducted by labeling the first-generation precursors of RO and OVOCs in the model.
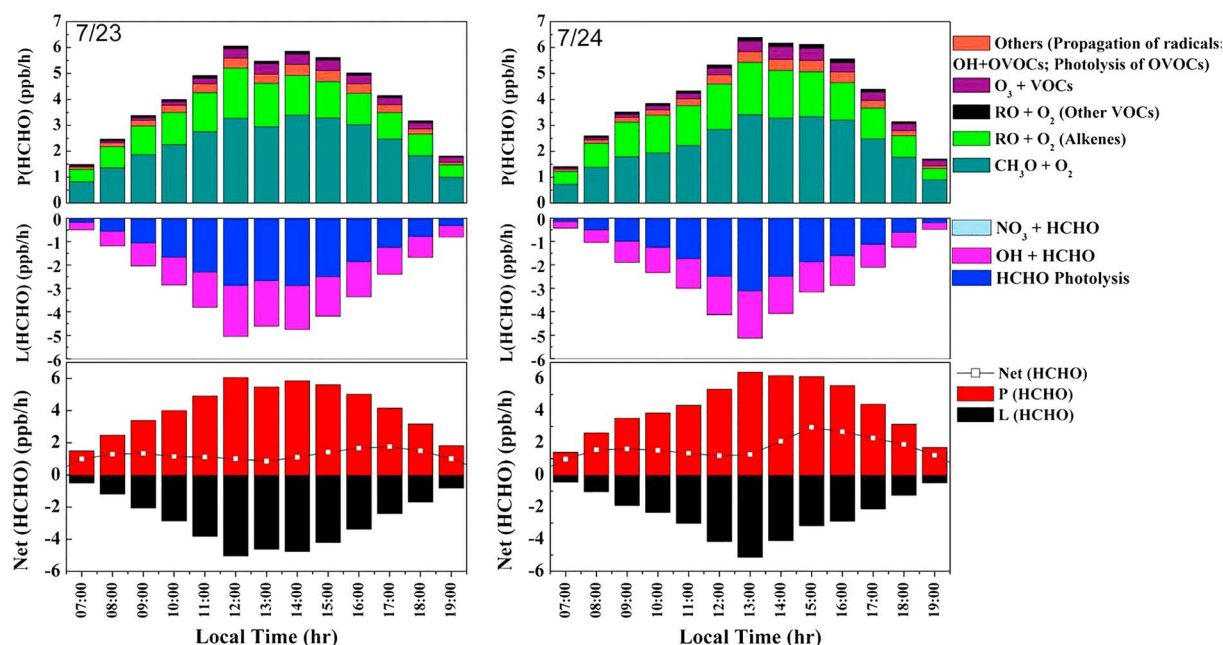
Figure 3. Model-simulated in situ HCHO production rate (P(HCHO)), destruction rate (L(HCHO)), net rate (Net(HCHO)), and breakdown of P(HCHO) and L(HCHO) on 23 and 24 July 2008.

Figures 3–6 illustrate the detailed formation and loss pathways of HCHO, CH_3CHO, CHOCHO, and MGLY during the two cases. Overall, the formation and loss processes of carbonyls were consistent for each case but differed among carbonyl species. On average, HCHO production was dominated by the reactions of $RO + O_2$, accounting for 87% and 88% of the total production rate on 23 and 24 July, respectively. The $O_3 + OVOC$ reactions and other reaction pathways (including radical propagation reactions, OVOC photolysis, and OH + OVOC reactions) made only minor contributions (<7%) (see Figure 3). Further classification of the $RO + O_2$ pathway revealed that the reaction of $CH_3O + O_2$ alone made an important contribution (56% and 53%), followed by RO produced by alkenes including biogenic hydrocarbons (29% and 32%). Overall, the
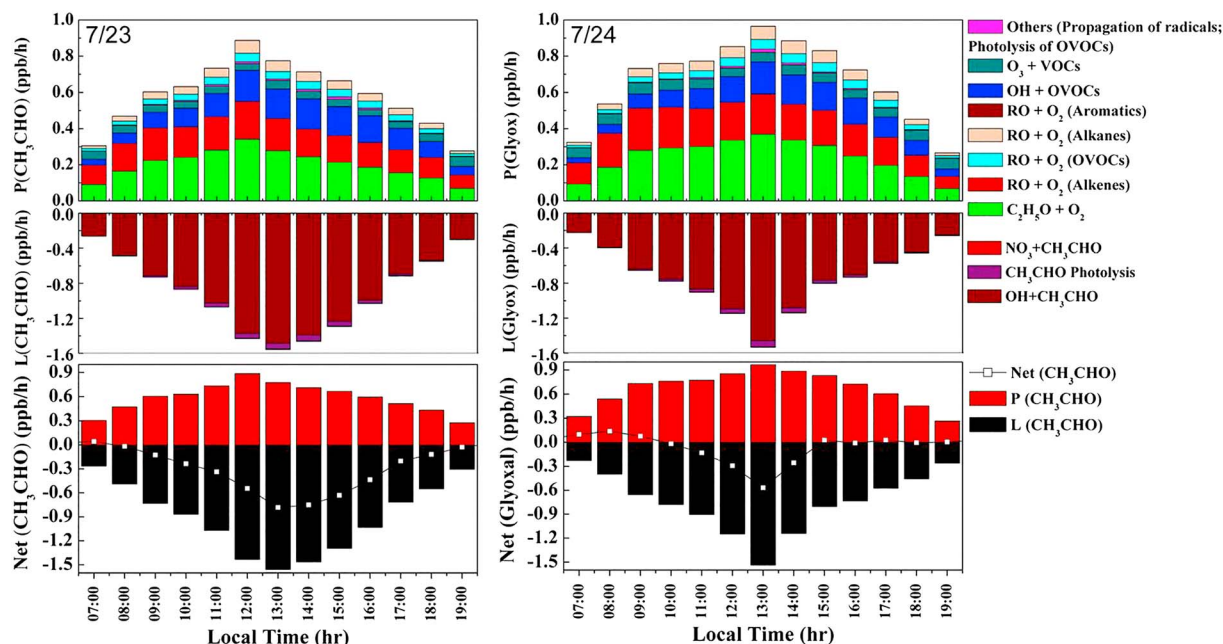
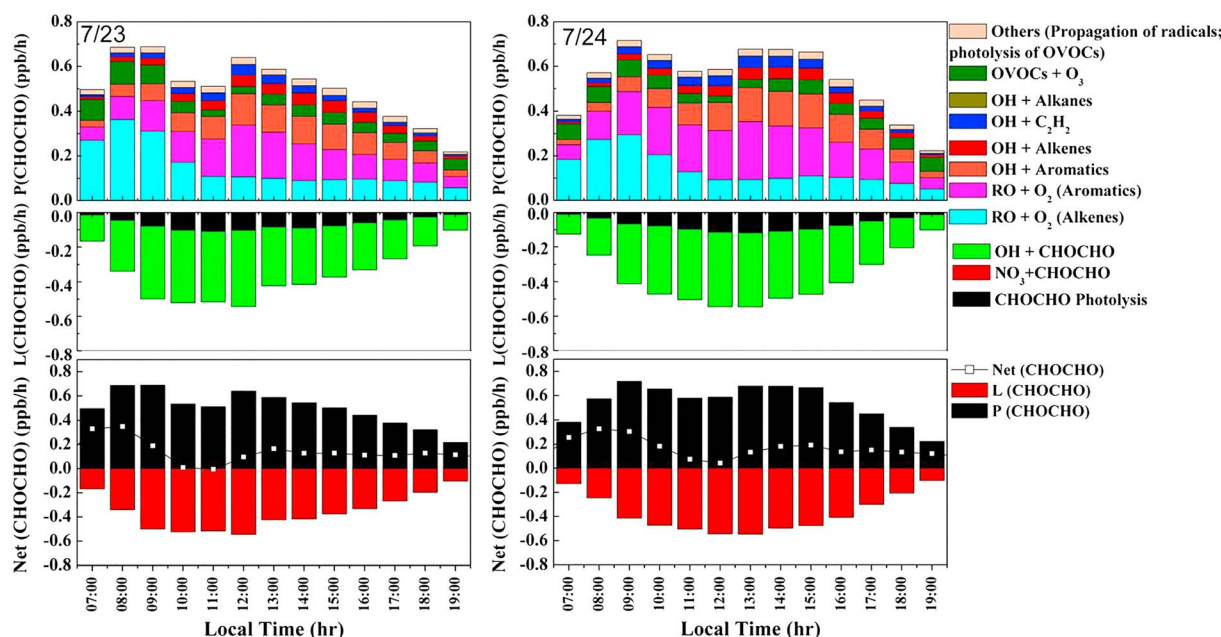**Figure 4.** The same as Figure 3 but for CH_3CHO.

Figure 5. The same as Figure 3 but for CHOCHO.

modeled explicit HCHO chemistry underlined the important role of alkene hydrocarbons in the secondary formation of HCHO, which was in good agreement with previous reports by Liu et al. (2015).

The reactions of RO with O_2 dominated the CH_3CHO production (72% and 74% for each case), followed by the reactions of OH + OVOCs (19% and 15%), O_3 + OVOCs (8% and 9%), and negligible levels of the other reactions (including radical propagation reactions and OVOC photolysis) (1% and 2% in total). Further classification of the control route (RO + O_2) suggested that the reactions of C_2H_5O + O_2 contributed 34% and 35% to the total production rate of CH_3CHO. In particular, RO produced by the oxidation of alkenes showed a comparable role (26% and 27%) to the C_2H_5O + O_2 reaction (see Figure 4). Hence, the oxidation of alkene hydrocarbons also contributed to an important proportion of the CH_3CHO production.
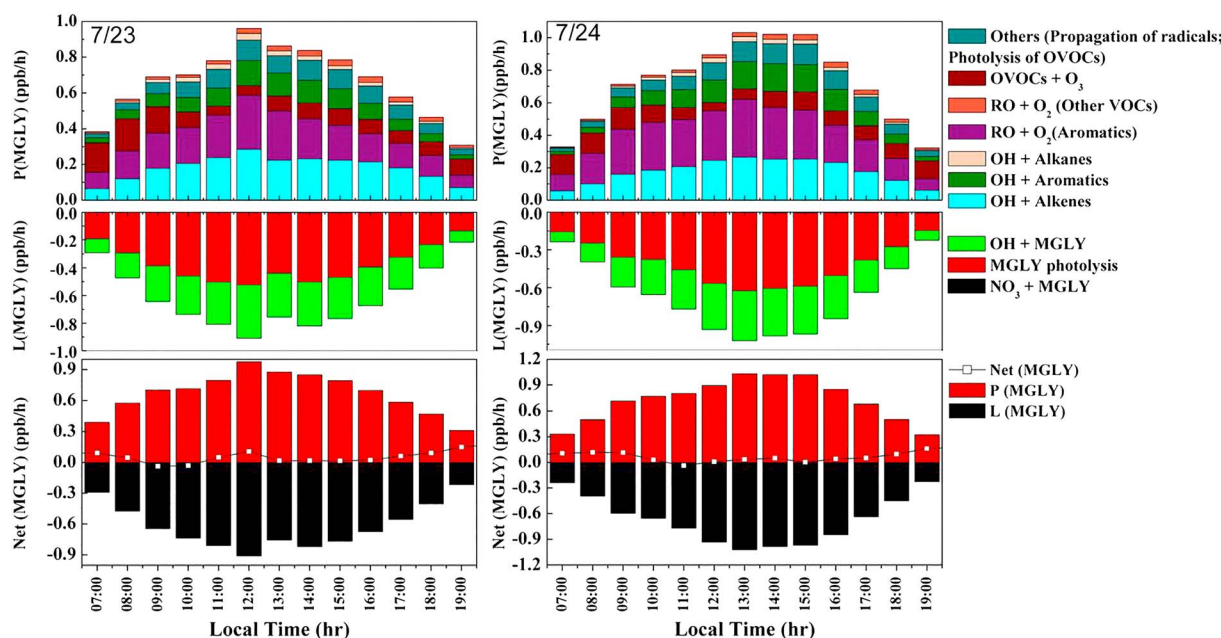

Figure 6. The same as Figure 3 but for MGLY.

For CHOCHO, the reactions of RO and O_2 were still the significant pathway (54% and 56%), with OH + OVOC reactions being another important formation route (29% and 28%), followed by O_3 + OVOC reactions (12% in both cases) (see Figure 5). The RO + O_2 reactions can be further categorized into two subtypes considering the different precursors of RO radicals. One of these subtypes is the reactions of RO produced by the oxidation of alkenes with O_2, which contributed 26% and 29% to the in situ formation of CHOCHO, and the other is the reactions of RO produced from aromatics with O_2 (28% and 27%). For the OH + OVOC reactions, there are also two subtypes. The OH-initiated oxidation of OVOCs produced from the oxidation of aromatics accounted for 17% and 16% of the CHOCHO formation, followed by the reactions of OVOCs formed from alkenes (7% in both cases). In addition, the OH + C_2H_2 reaction alone accounted for approximately 5% in both cases. Therefore, the aromatic VOCs contributed the most to the CHOCHO production (>43% in total). These results were in accordance with the satellite-based modeling analysis over the PRD region by Chan Miller et al. (2016), which suggested that the CHOCHO hot spot over the PRD can be ascribed to the emissions of aromatics.

The formation of MGLY was dominated by the reactions of OH + OVOCs (41% and 38%) and RO + O_2 (31% and 35%) (see Figure 6). The O_3 + OVOC reactions accounted for 17% and 16% for the two sampling dates, and other routes such as OVOC photolysis and radical propagation reactions were responsible for the remainder. The reactions of RO + O_2 and OH + OVOCs were further classified into a number of routes by tracking their parent precursors. Specifically, the RO radicals produced from aromatics accounted for 27% and 32%. The OH-initiated reactions of OVOCs formed from the oxidation of alkenes contributed 27% and 24%, followed by the OVOCs produced from aromatics (12% for both cases) and alkanes (2% for both cases). Statistically, the oxidation of alkenes and aromatics accounted for at least 24% and 39% of the MGLY secondary formation in Beijing.

Figures 3–6 also show the loss pathways and net rates for the target carbonyls. It can be clearly seen that the destruction pathways for these four carbonyls were essentially the same, and they were governed by the reactions with OH and photolysis. Specifically, the chemical losses of HCHO and MGLY were under the combined control of both reactions with OH and photolysis. In contrast, the CH_3CHO and CHOCHO losses were mainly governed by the reactions with OH. The daytime average (07:00 to 18:00 LT) net production rates of HCHO, CHOCHO, and MGLY were estimated as 1.04 to 1.32, 0.11 to 0.13, and 0.05 to 0.06 ppb h^{-1}, respectively. However, it is noteworthy that the CH_3CHO production was significantly lower than the CH_3CHO destruction in both cases, implying the net chemical loss of CH_3CHO. The CH_3CHO observed in this study was strongly associated with primary sources and regional residuals, and the in situ photochemistry could have a negative effect on the accumulation of CH_3CHO (Altemose et al., 2015).

3.2.2. Identification of Key Precursor Species

The aforementioned analyses indicated the significant roles of alkenes and aromatics in the secondary formation of carbonyls in Beijing. In this section, we further identify the key precursors by calculating the relative incremental reactivity (RIR), which has been applied in many previous studies (Xue, Wang, Gao, et al., 2014; Xue, Wang, Wang, et al., 2014). More than 50 hydrocarbon species were categorized into five subgroups: alkenes, biogenic hydrocarbons (BHC, including isoprene, α-pinene, and β-pinene in this study), C_4HC (alkanes with four or more carbons), aromatics, and less reactive hydrocarbons (LRHC, including ethane, propane, ethyne, and methane in this study) (Xue, Wang, Gao, et al., 2014).

Figure 7 shows the calculated RIRs of the major VOC groups for the carbonyl formation. It can be clearly seen that the RIR results were quite similar for the two cases. Overall, the RIRs for these five groups were all positive, revealing that reducing their emissions would effectively mitigate the carbonyl pollution in Beijing. In particular, the HCHO production was mainly controlled by BHC and anthropogenic alkenes with the highest RIR values, which agrees with the previous study in Beijing (Liu et al., 2015). With regard to CH_3CHO, it is interesting to note that in addition to anthropogenic alkenes, which were a significant contributor, C_4HC also played an important role in the secondary formation of CH_3CHO. In terms of CHOCHO, aromatics and BHC presented the highest RIR values, suggesting that these species played the dominant role in the CHOCHO formation in Beijing. Therefore, cutting the emissions of aromatic VOCs would be an effective method to reduce the levels of CHOCHO and thus O_3 and aerosol pollution in Beijing. In terms of MGLY, BHC, aromatics, and alkenes all showed high RIR values, indicating that control of the emissions of aromatics and alkenes should be efficient for the abatement of MGLY production in Beijing.
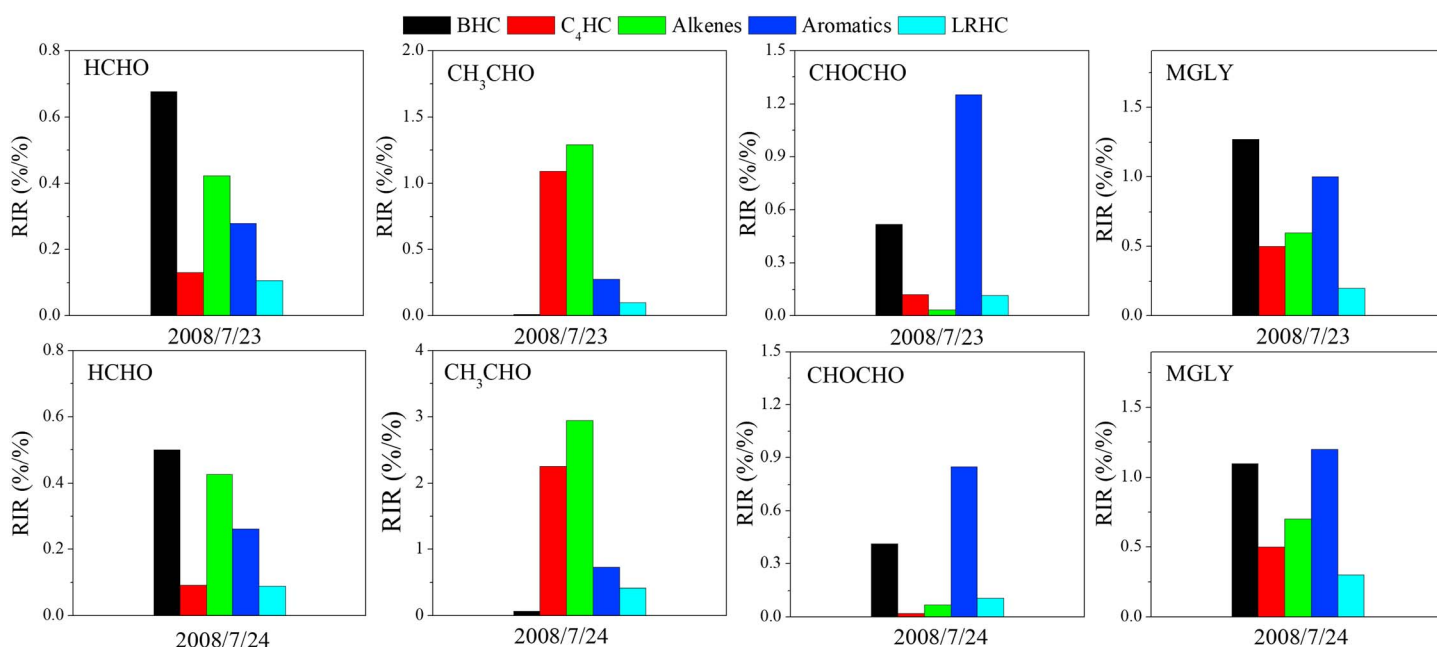
Figure 7. The model-calculated RIRs of the five major VOC groups for the secondary formation of major carbonyls on 23 and 24 July 2008.

With the explicit mechanism of MCM, the OBM-AOCP model is capable of identifying the carbonyl precursors at the species level and quantifying the relationships between carbonyl species and their precursors. To investigate the relative contribution of the individual VOC species (in total 50 species were identified in this study) to the formation of carbonyls, a series of sensitivity model simulations were further conducted. Figure 8 shows the top 10 VOC species with the highest RIR values. For HCHO, two alkene compounds,
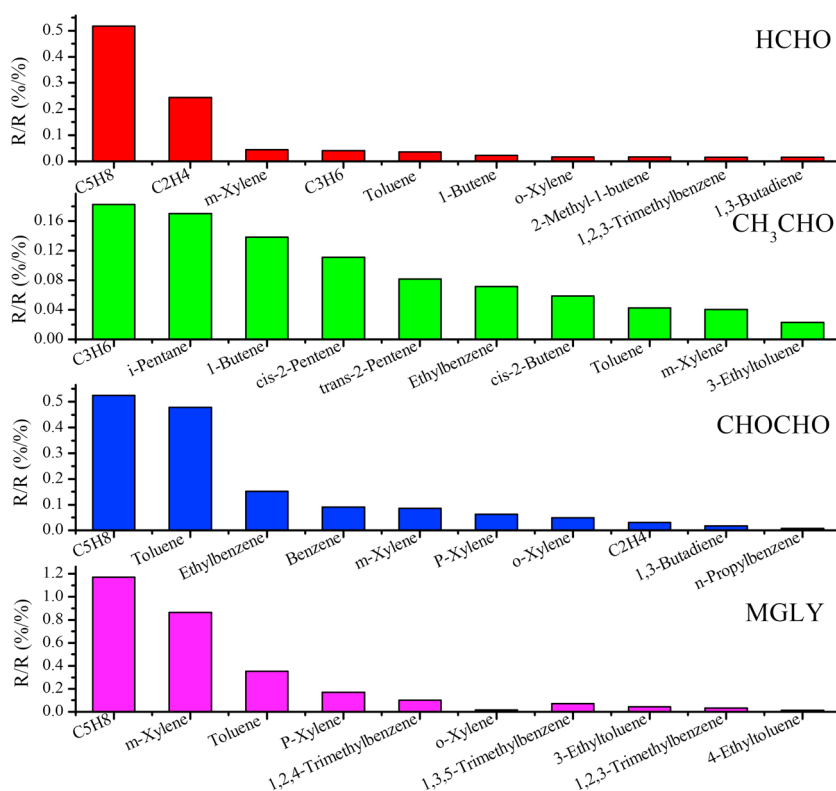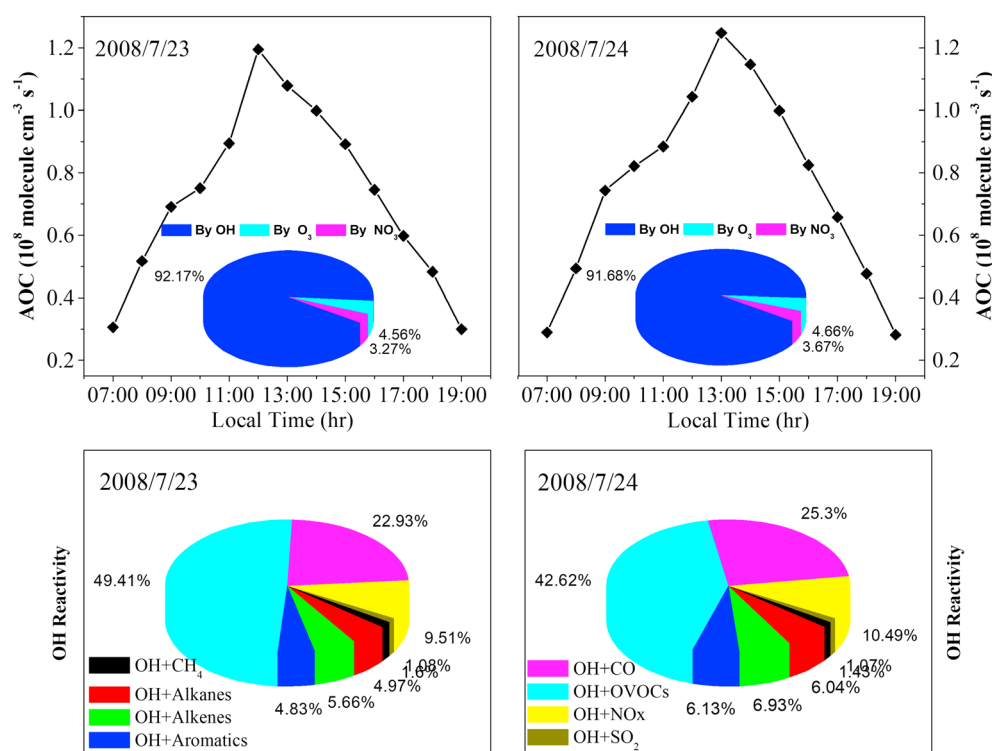

**Figure 8.** Average RIR values of the individual top 10 VOC species for carbonyl formation in Beijing.

Figure 9. Times series of the model-simulated AOC and budget of the OH reactivity on 23 and 24 July 2008.

isoprene (C_5H_8) and ethene (C_2H_4), were found to dominate the total RIR value of VOCs, indicating that the local HCHO formation in Beijing is mainly attributable to C_5H_8 and C_2H_4. This suggests that reducing anthropogenic emissions of C_2H_4 would reduce the HCHO pollution. In comparison, for CH_3CHO, propene (C_3H_6), i-butene, cis-2-pentene, and i-pentane showed the highest RIR values, which is consistent with previous results suggesting that alkenes and alkanes were the main precursors of CH_3CHO at an urban site in Beijing (Liu et al., 2015). In terms of CHOCHO, in addition to C_5H_8 showing the highest RIR, anthropogenic aromatics, especially toluene, also presented a significant contribution. For MGLY, C_5H_8 and another aromatic compound, m-xylene, showed the highest RIR values. Overall, the dominant primary precursors were quite inhomogeneous for the various carbonyls, indicating that various control strategies should be in place to mitigate various carbonyl compounds.

3.3. Impacts on AOC, RO$_x$ Budget, and O$_3$ Formation

AOC calculations were conducted to investigate the potential role of carbonyls in the atmospheric oxidizing capacity in Beijing during the photochemical smog episodes. Briefly, AOC was calculated by summing the total reaction rates of CH_4, CO, SO_2, NO_x, and VOCs oxidized by OH, O_3, and NO_3, respectively. A detailed description can be found elsewhere (Xue et al., 2015, 2016). The time series of the model-simulated AOC and the corresponding AOC composition profiles for 23 and 24 July 2008 are illustrated in Figure 9. Generally, the AOC showed prominent peaks at noon (~1.32×10^8 and 1.45×10^8 molecules cm^{-3} s^{-1} for the 2 days). The daytime average values of AOC were 7.36×10^7 and 7.72×10^7 molecules cm^{-3} s^{-1} on 23 and 24 July, respectively. These levels are comparable to those determined at Tung Chung in Hong Kong, southern China (Xue et al., 2016). As seen in Figure 9, OH was the dominant oxidant, contributing to 92% of the AOC in both cases. To further assess the OH oxidation, the OH reactivity composition profiles for different VOCs (not only the measured species but also the modeled intermediates), CO, SO_2, and NO_x were also calculated (see Figure 9, bottom). It is clear that the oxidation of OVOCs (mainly carbonyls) contributed the most to the OH reactivity (i.e., 49% and 43% for each case). In addition, oxidation of CO contributed on average 23% and 25% for both cases, with SO_2, NO_x, alkanes, alkenes, and aromatics each accounting for 4% to 10% of the OH reactivity. These results are similar to the previous studies in Hong Kong and the PRD
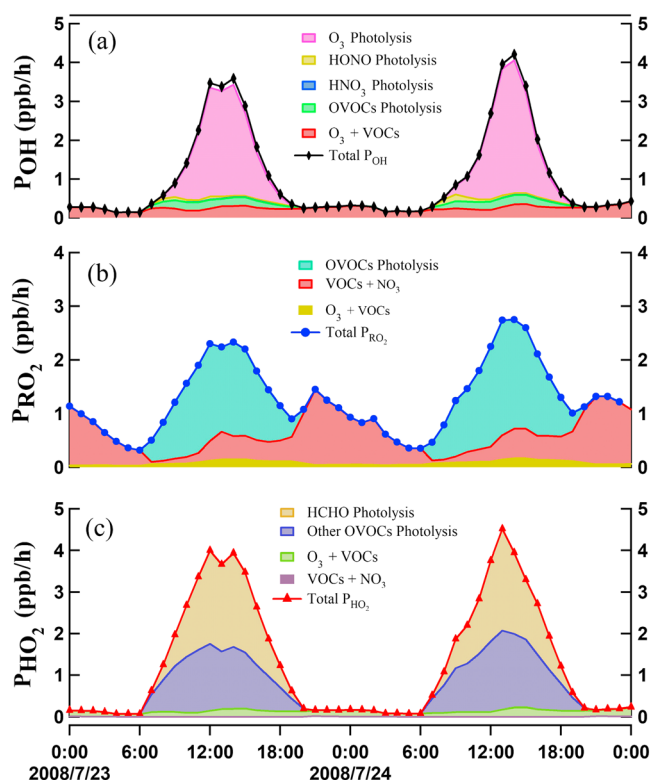
Figure 10. Breakdown of (a) P_{OH}, (b) P_{RO2}, and (c) P_{HO2} at CRAES on 23 and 24 July 2008.

region (Xue et al., 2016), which underlined the dominant role of carbonyls in OH reactivity and the atmospheric oxidizing capacity.

The RO_x chemistry was also elucidated using the OBM-AOCP model. Figures 10a–10c show the breakdown of OH, RO_2, and HO_2 production rates (P_{OH}, P_{RO2}, and P_{HO2}) for the two dates. O_3 photolysis was the predominant OH source with daytime average production rates of 1.19 and 1.21 ppb h^{-1} on 23 and 24 July, respectively. The remaining primary OH sources, including HONO, OVOCs, and HNO_3 photolysis and O_3 + VOC reactions, accounted for relatively minor contributions. It should be noted that HONO was not measured in this study but predicted by the box model. Some recent studies have indicated that the current models generally cannot explain the measured ambient HONO concentrations (Liu, Wang, Gu, et al., 2012); thus, the estimated contribution of HONO photolysis in the present study is expected to be underestimated. For HO_2, 56% to 61% of its primary production was from HCHO photolysis, with mean production rates of 1.21 and 1.06 ppb h^{-1} in the daytime, and 31% to 35% was from photolysis of other OVOCs with mean production rates of 0.63 and 0.66 ppb h^{-1}. These results are generally in line with those calculated in the polluted areas of Hong Kong (Xue et al., 2016) and Beijing (Liu, Wang, Gu, et al., 2012). In comparison, for RO_2, the photolysis of OVOCs contributed the most (74% and 73%) during the daytime with mean production rates of 1.16 and 1.25 ppb h^{-1} on 23 and 24 July, respectively. Furthermore, the VOCs + NO_3 reactions were found to be not only the second most important source of RO_2 throughout the daytime (19% and 22%) but also the biggest contributor of RO_2 at night (94% and 92%), indicating the important role of NO_3 in the AOC in the polluted atmosphere. In general, the high contributions of NO_3 radical are mainly attributed to the high abundances of O_3 and NO_2 (Xue et al., 2016). Overall, this analysis of the radical budget highlighted the important role of OVOCs in the primary production of HO_2 and RO_2 and hence the initiation of atmospheric oxidation chemistry.
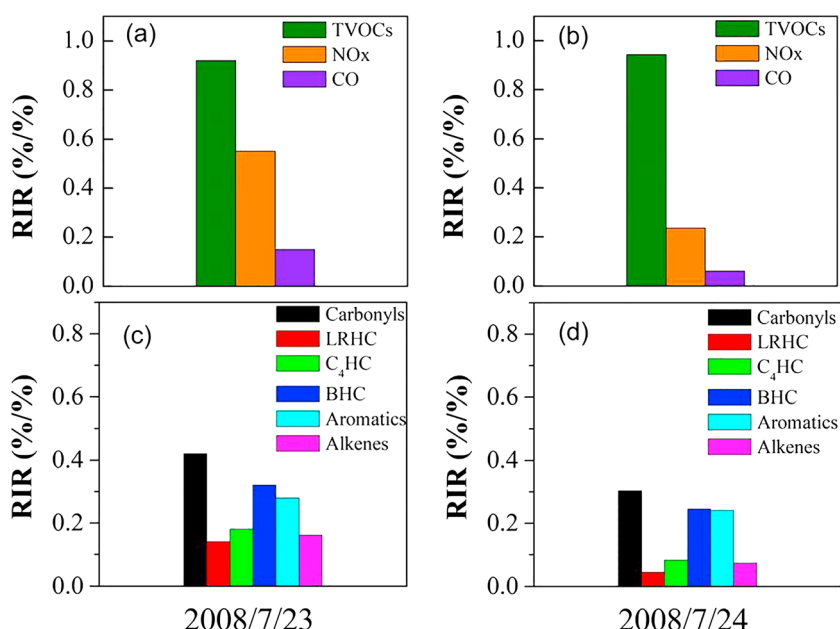
Figure 11. The model-calculated RIRs for major O_3 precursors and the VOC groups on 23 and 24 July 2008.

As mentioned above, severe O_3 pollution was encountered in Beijing during the early sampling period. To understand the O_3 formation regimes, we also performed sensitivity model simulations to determine the O_3-precursor relationships. The results are summarized in Figure 11. It can be seen that TVOCs (total VOCs, including carbonyls), NO_x, and CO all showed positive RIR values, indicating that the in situ O_3 formation in Beijing was under a mixed-control regime. This result is consistent with that of Liu, Wang, Gu, et al. (2012), which indicated a transition regime of O_3 formation at an urban site in Beijing. Moreover, the RIR of TVOCs was much higher than those of NO_x and CO, which reveals that cutting VOC emissions would be more effective for controlling O_3 pollution. In addition, to further reveal the effects of the VOC subgroups, including carbonyls (only the measured carbonyl species), BHC, alkenes, aromatics, C_4HC, and LRHC, on O_3 formation, their corresponding RIR values were also calculated (see Figures 11c and 11d). It can be clearly seen that carbonyls exhibited the greatest RIR values (i.e., 0.42 and 0.30) for the two cases, suggesting their dominant role in O_3 production in Beijing. Overall, these analyses reveal the important contributions of carbonyls to the atmospheric photochemistry and O_3 formation in the polluted atmosphere of Beijing and demonstrate the urgent need for further understanding of the pollution characteristics and sources of carbonyls in the urban areas of China.

4. Conclusions

Our field experiments performed at a suburban site of Beijing in the summer of 2008 revealed severe photochemical air pollution accompanied by high concentrations of carbonyls and O_3, which provided an opportunity to probe the photochemistry of the polluted atmosphere. During the investigation, in addition to high levels of HCHO, acetone, and CH_3CHO, CHOCHO and MGLY also showed relatively abundant concentrations. Secondary formation was found to be an important source of these abundant carbonyls. The reactions of $RO + O_2$ and/or $OH + OVOCs$ dominated the photochemical formation of carbonyls. Specifically, the oxidation of alkenes (mainly C_5H_8 and C_2H_4) is the major formation route of HCHO. The degradation of alkenes, such as C_3H_6, i-butene, and cis-2-pentene, and that of alkanes, predominantly i-pentane, played an important role in the CH_3CHO formation. The oxidation of isoprene and aromatics dominated the secondary formation of CHOCHO and MGLY. Therefore, reducing the emissions of alkenes and aromatics should be an efficient way to mitigate carbonyl formation and thus O_3 and secondary aerosol pollution in Beijing.

Strong atmospheric oxidizing capacity was predicted (7.36 to 7.72×10^7 molecules cm^{-3} s^{-1}) during the smog episodes, with OH contributing to approximately 92% of the daytime oxidation. The photolysis of OVOCs was the dominant primary RO_x source. Sensitivity analyses showed that O_3 production was under a mixed-control regime with OVOCs (mainly carbonyls) being the key species. Overall, this study underlined the important role of carbonyls in photochemical reactions, oxidative capacity, and radical chemistry in the polluted atmosphere of Beijing and provided insights into carbonyl pollution and its formation mechanisms. The findings of this study will be helpful in the development of effective control strategies to mitigate the severe photochemical air pollution in Beijing and other polluted areas of China.

References

Altemose, B., Gong, J., Zhu, T., Hu, M., Zhang, L., Cheng, H., … Strickland, P. O. (2015). Aldehydes in relation to air pollution sources: A case study around the Beijing Olympics. *Atmospheric Environment*, *109*, 61–69. https://doi.org/10.1016/j.atmosenv.2015.02.056

Atkinson, R. (2000). Atmospheric chemistry of VOCs and NO_x. *Atmospheric Environment*, *34*(12-14), 2063–2101. https://doi.org/10.1016/S1352-2310(99)00460-4

Chan Miller, C., Jacob, D. J., González Abad, G., & Chance, K. (2016). Hotspot of glyoxal over the Pearl River delta seen from the OMI satellite instrument: Implications for emissions of aromatic hydrocarbons. *Atmospheric Chemistry and Physics*, *16*(7), 4631–4639. https://doi.org/10.5194/acp-16-4631-2016

Cheng, H., Guo, H., Wang, X., Saunders, S. M., Lam, S. H., Jiang, F., … Ho, K. F. (2010). On the relationship between ozone and its precursors in the Pearl River Delta: Application of an observation-based model (OBM). *Environmental Science and Pollution Research International*, *17*(3), 547–560. https://doi.org/10.1007/s11356-009-0247-9

Chou, C. C. K., Tsai, C. Y., Chang, C. C., Lin, P. H., Liu, S. C., & Zhu, T. (2011). Photochemical production of ozone in Beijing during the 2008 Olympic Games. *Atmospheric Chemistry and Physics*, *11*(18), 9825–9837. https://doi.org/10.5194/acp-11-9825-2011

Duan, J., Guo, S., Tan, J., Wang, S., & Chai, F. (2012). Characteristics of atmospheric carbonyls during haze days in Beijing, China. *Atmospheric Research*, *114-115*, 17–27. https://doi.org/10.1016/j.atmosres.2012.05.010

Fu, T. M., Jacob, D. J., Wittrock, F., Burrows, J. P., Vrekoussis, M., & Henze, D. K. (2008). Global budgets of atmospheric glyoxal and methylglyoxal, and implications for formation of secondary organic aerosols. *Journal of Geophysical Research*, *113*, D15303. https://doi.org/10.1029/2007JD009505

Guo, S., Chen, M., & Tan, J. (2016). Seasonal and diurnal characteristics of atmospheric carbonyls in Nanning, China. *Atmospheric Research*, *169*, 46–53. https://doi.org/10.1016/j.atmosres.2015.09.028

Ho, K. F., Ho, S. S., Dai, W. T., Cao, J. J., Huang, R. J., Tian, L., & Deng, W. J. (2014). Seasonal variations of monocarbonyl and dicarbonyl in urban and sub-urban sites of Xi'an, China. *Environmental Monitoring and Assessment*, *186*(5), 2835–2849. https://doi.org/10.1007/s10661-013-3584-6

Ho, S. S. H., & Yu, J. Z. (2004). Determination of airborne carbonyls: Comparison of a thermal desorption/GC method with the standard DNPH/HPLC method. *Environmental Science & Technology*, *38*(3), 862–870. https://doi.org/10.1021/es034795w

Hofzumahaus, A., Rohrer, F., Lu, K., Bohn, B., Brauers, T., Chang, C. C., … Li, X. (2009). Amplified trace gas removal in the troposphere. *Science*, *324*(5935), 1702–1704. https://doi.org/10.1126/science.1164566

Huang, S., Shao, M., Lu, S., & Liu, Y. (2008). Reactivity of ambient volatile organic compounds (VOCs) in summer of 2004 in Beijing. *Chinese Chemical Letters*, *19*(5), 573–576. https://doi.org/10.1016/j.cclet.2008.03.029

Huang, Y., Ho, S. S., Ho, K. F., Lee, S. C., Yu, J. Z., & Louie, P. K. (2011). Characteristics and health impacts of VOCs and carbonyls associated with residential cooking activities in Hong Kong. *Journal of Hazardous Materials*, *186*(1), 344–351. https://doi.org/10.1016/j.jhazmat.2010.11.003

Jenkin, M. E., Saunders, S. M., Wagner, V., & Pilling, M. J. (2003). Protocol for the development of the Master Chemical Mechanism, MCM v3 (Part B): Tropospheric degradation of aromatic volatile organic compounds. *Atmospheric Chemistry and Physics*, *3*(1), 181–193. https://doi.org/10.5194/acp-3-181-2003

Jenkin, M. E., Young, J. C., & Rickard, A. R. (2015). The MCM v3. 3 degradation scheme for isoprene. *Atmospheric Chemistry and Physics Discussions*, *15*(6), 9709–9766. https://doi.org/10.5194/acpd-15-9709-2015

Li, X., Rohrer, F., Brauers, T., Hofzumahaus, A., Lu, K., Shao, M., … Wahner, A. (2014). Modeling of HCHO and CHOCHO at a semi-rural site in southern China during the PRIDE-PRD2006 campaign. *Atmospheric Chemistry and Physics*, *14*(22), 12,291–12,305. https://doi.org/10.5194/acp-14-12291-2014

Li, Y., Shao, M., Lu, S., Chang, C. C., & Dasgupta, P. K. (2010). Variations and sources of ambient formaldehyde for the 2008 Beijing Olympic games. *Atmospheric Environment*, *44*(21-22), 2632–2639. https://doi.org/10.1016/j.atmosenv.2010.03.045

Lim, Y. B., Tan, Y., & Turpin, B. J. (2013). Chemical insights, explicit chemistry, and yields of secondary organic aerosol from OH radical oxidation of methylglyoxal and glyoxal in the aqueous phase. *Atmospheric Chemistry and Physics*, *13*(17), 8651–8667. https://doi.org/10.5194/acp-13-8651-2013

Ling, Z., Guo, H., Chen, G., Lam, S. H. M., & Fan, S. (2016). Formaldehyde and acetaldehyde at different elevations in mountainous areas in Hong Kong. *Aerosol and Air Quality Research*, *16*(8), 1868–1878. https://doi.org/10.4209/aaqr.2015.09.0571

Liu, Y., Shao, M., Kuster, W. C., Goldan, P. D., Li, X., Lu, S., & de Gouw, J. A. (2009). Source identification of reactive hydrocarbons and oxygenated VOCs in the summertime in Beijing. *Environmental Science & Technology*, *43*(1), 75–81. https://doi.org/10.1021/es801716n

Liu, Y., Yuan, B., Li, X., Shao, M., Lu, S., Li, Y., … He, L. (2015). Impact of pollution controls in Beijing on atmospheric oxygenated volatile organic compounds (OVOCs) during the 2008 Olympic Games: Observation and modeling implications. *Atmospheric Chemistry and Physics*, *15*(6), 3045–3062. https://doi.org/10.5194/acp-15-3045-2015

Liu, Z., Wang, Y., Gu, D., Zhao, C., Huey, L. G., Stickel, R., … Liu, S. C. (2010). Evidence of reactive aromatics as a major source of peroxy acetyl nitrate over China. *Environmental Science & Technology*, *44*(18), 7017–7022. https://doi.org/10.1021/es1007966

Liu, Z., Wang, Y., Gu, D., Zhao, C., Huey, L. G., Stickel, R., … Amoroso, A. (2012). Summertime photochemistry during CAREBeijing-2007: RO_x budgets and O_3 formation. *Atmospheric Chemistry and Physics*, *12*(16), 7737–7752. https://doi.org/10.5194/acp-12-7737-2012

Liu, Z., Wang, Y., Vrekoussis, M., Richter, A., Wittrock, F., Burrows, J. P., … Chen, C. (2012). Exploring the missing source of glyoxal (CHOCHO) over China. *Geophysical Research Letters*, *39*, L10812. https://doi.org/10.1029/2012GL051645

Lü, H., Cai, Q. Y., Wen, S., Chi, Y., Guo, S., Sheng, G., … Antizar-Ladislao, B. (2009). Carbonyl compounds in the ambient air of hazy days and clear days in Guangzhou, China. *Atmospheric Research*, *94*(3), 363–372. https://doi.org/10.1016/j.atmosres.2009.06.014

Lu, K. D., Hofzumahaus, A., Holland, F., Bohn, B., Brauers, T., Fuchs, H., … Kondo, Y. (2013). Missing OH source in a suburban environment near Beijing: Observed and modelled OH and HO_2 concentrations in summer 2006. *Atmospheric Chemistry and Physics*, *13*(2), 1057–1080. https://doi.org/10.5194/acp-13-1057-2013

Mason, S. A., Field, R. J., Yokelson, R. J., Kochivar, M. A., Tinsley, M. R., Ward, D. E., & Hao, W. M. (2001). Complex effects arising in smoke plume simulations due to inclusion of direct emissions of oxygenated organic species from biomass combustion. *Journal of Geophysical Research*, *106*(D12), 12,527–12,539. https://doi.org/10.1029/2001JD900003

Rao, Z., Chen, Z., Liang, H., Huang, L., & Huang, D. (2016). Carbonyl compounds over urban Beijing: Concentrations on haze and non-haze days and effects on radical chemistry. *Atmospheric Environment*, *124*, 207–216. https://doi.org/10.1016/j.atmosenv.2015.06.050

Saunders, S. M., Jenkin, M. E., Derwent, R. G., & Pilling, M. J. (2003). Protocol for the development of the Master Chemical Mechanism, MCMv3 (Part A): Tropospheric degradation of non-aromatic volatile organic compounds. *Atmospheric Chemistry and Physics*, *3*(1), 161–180. https://doi.org/10.5194/acp-3-161-2003

Simpson, I. J., Blake, N. J., Barletta, B., Diskin, G. S., Fuelberg, H. E., Gorham, K., … Weinheimer, A. J. (2010). Characterization of trace gases measured over Alberta oil sands mining operations: 76 speciated C2–C10 volatile organic compounds (VOCs), CO_2, CH_4, CO, NO, NO_2, NO_y, O_3 and SO_2. *Atmospheric Chemistry and Physics*, *10*(23), 11,931–11,954. https://doi.org/10.5194/acp-10-11931-2010

Tan, Z., Fuchs, H., Lu, K., Hofzumahaus, A., Bohn, B., Broch, S., … Holland, F. (2017). Radical chemistry at a rural site (Wangdu) in the North China Plain: Observation and model calculations of OH, HO_2 and RO_2 radicals. *Atmospheric Chemistry and Physics*, *17*(1), 663–690. https://doi.org/10.5194/acp-17-663-2017

Tham, Y. J., Wang, Z., Li, Q., Yun, H., Wang, W., Wang, X., … Wang, T. (2017). Significant concentrations of nitryl chloride sustained in the morning: Investigations of the causes and impacts on ozone production in a polluted region of northern China. *Atmospheric Chemistry and Physics*, *16*, 14,959–14,977.

Wang, M., Chen, W., Shao, M., Lu, S., Zeng, L., & Hu, M. (2015). Investigation of carbonyl compound sources at a rural site in the Yangtze River Delta region of China. *Journal of Environmental Sciences*, *28*, 128–136. https://doi.org/10.1016/j.jes.2014.12.001

Wang, T., Cheung, V. T., Anson, M., & Li, Y. S. (2001). Ozone and related gaseous pollutants in the boundary layer of eastern China: Overview of the recent measurements at a rural site. *Geophysical Research Letters*, *28*(12), 2373–2376. https://doi.org/10.1029/2000GL012378

Wang, T., Ding, A., Gao, J., & Wu, W. S. (2006). Strong ozone production in urban plumes from Beijing, China. *Geophysical Research Letters*, *33*, L21806. https://doi.org/10.1029/2006GL027689

Wang, T., Nie, W., Gao, J., Xue, L. K., Gao, X. M., Wang, X., … Wang, S. L. (2010). Air quality during the 2008 Beijing Olympics: Secondary pollutants and regional impact. *Atmospheric Chemistry and Physics*, *10*(16), 7603–7615. https://doi.org/10.5194/acp-10-7603-2010

Wang, T., Xue, L., Brimblecombe, P., Lam, Y. F., Li, L., & Zhang, L. (2016). Ozone pollution in China: A review of concentrations, meteorological influences, chemical precursors, and effects. *Science of the Total Environment*, *575*, 1582–1596. https://doi.org/10.1016/j. scitotenv.2016.10.081

Xu, J., Ma, J. Z., Zhang, X. L., & Xu, X. B. (2011). Measurements of ozone and its precursors in Beijing during summertime: Impact of urban plumes on ozone pollution in downwind rural areas. *Atmospheric Chemistry and Physics*, *11*(23), 12,241–12,252. https://doi.org/10.5194/ acp-11-12241-2011

Xue, L., Wang, T., Wang, X., Blake, D. R., Gao, J., Nie, W., … Ding, A. (2014). On the use of an explicit chemical mechanism to dissect peroxy acetyl nitrate formation. *Environmental Pollution*, *195*(36), 39–47. https://doi.org/10.1016/j.envpol.2014.08.005

Xue, L. K., Gu, R. R., Wang, T., Wang, X., Saunders, S., Blake, D., … Xu, Z. (2016). Oxidative capacity and radical chemistry in the polluted atmosphere of Hong Kong and Pearl River Delta region: Analysis of a severe photochemical smog episode. *Atmospheric Chemistry and Physics*, *16*(15), 9891–9903. https://doi.org/10.5194/acp-16-9891-2016

Xue, L. K., Saunders, S. M., Wang, T., Gao, R., Wang, X. F., Zhang, Q. Z., & Wang, W. X. (2015). Development of a chlorine chemistry module for the Master Chemical Mechanism. *Geoscientific Model Development*, *8*(10), 3151–3162. https://doi.org/10.5194/gmd-8-3151-2015

Xue, L. K., Wang, T., Gao, J., Ding, A. J., Zhou, X. H., Blake, D. R., … Zhang, Q. Z. (2014). Ground-level ozone in four Chinese cities: Precursors, regional transport and heterogeneous processes. *Atmospheric Chemistry and Physics*, *14*(23), 13,175–13,188. https://doi.org/10.5194/acp-14-13175-2014

Xue, L. K., Wang, T., Guo, H., Blake, D. R., Tang, J., Zhang, X. C., … Wang, W. X. (2013). Sources and photochemistry of volatile organic compounds in the remote atmosphere of western China: Results from the Mt. Waliguan Observatory. *Atmospheric Chemistry and Physics*, *13*(17), 8551–8567. https://doi.org/10.5194/acp-13-8551-2013

Xue, L. K., Wang, T., Louie, P. K., Luk, C. W., Blake, D. R., & Xu, Z. (2014). Increasing external effects negate local efforts to control ozone air pollution: A case study of Hong Kong and implications for other Chinese cities. *Environmental Science & Technology*, *48*(18), 10,769–10,775. https://doi.org/10.1021/es503278g

Xue, L. K., Wang, T., Zhang, J. M., Zhang, X. C., Poon, C. N., Ding, A. J., … Wang, W. X. (2011). Source of surface ozone and reactive nitrogen speciation at mount Waliguan in western China: New insights from the 2006 summer study. *Journal of Geophysical Research*, *116*, D07306. https://doi.org/10.1029/2010JD014735

Yang, X., Xue, L., Yao, L., Li, Q., Wen, L., Zhu, Y., … Lee, S. (2017). Carbonyl compounds at Mount Tai in the North China Plain: Characteristics, sources, and effects on ozone formation. *Atmospheric Research*, *196*, 53–61. https://doi.org/10.1016/j.atmosres.2017.06.005

Yuan, B., Shao, M., Gouw, J., Parrish, D. D., Lu, S., Wang, M., … Hu, M. (2012). Volatile organic compounds (VOCs) in urban air: How chemistry affects the interpretation of positive matrix factorization (PMF) analysis. *Journal of Geophysical Research*, *117*, D24302. https://doi.org/ 10.1029/2012JD08236

Zhang, L., Brook, J. R., & Vet, R. (2003). A revised parameterization for gaseous dry deposition in air-quality models. *Atmospheric Chemistry and Physics*, *3*(6), 2067–2082. https://doi.org/10.5194/acp-3-2067-2003